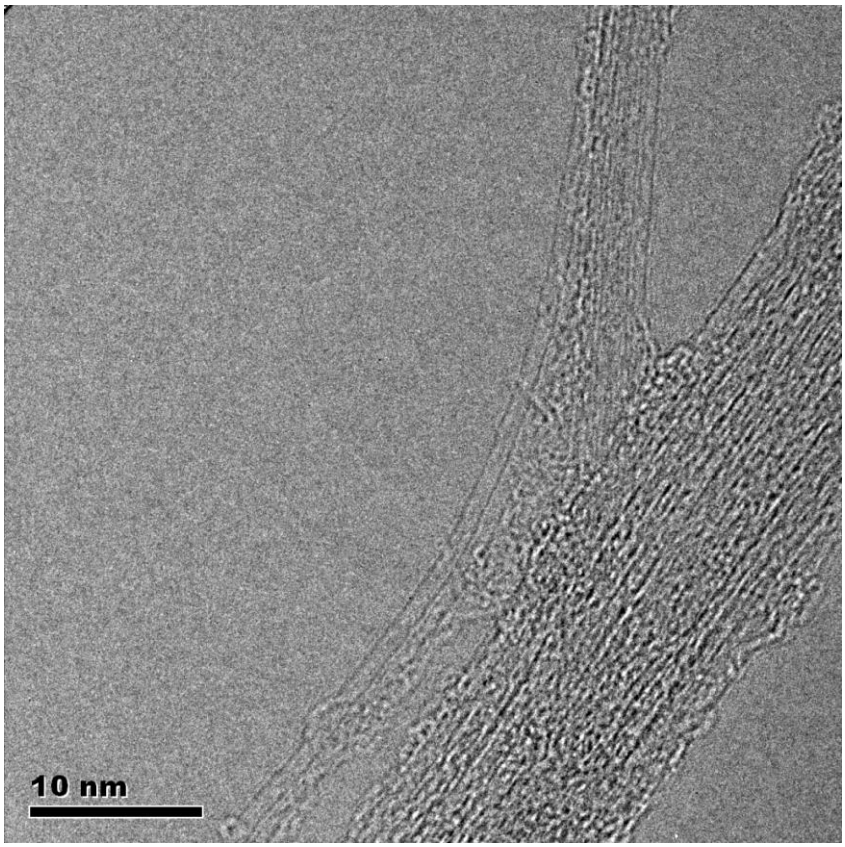

Supplementary Figure S1 | A typical HRTEM image of purified SWCNTs. The HRTEM sample was prepared by sonicating purified SWCNTs in ethanol. The suspension was deposited onto a lacey support film, and then dried in air. The imaging was carried out on a HRTEM Tecnai F20.

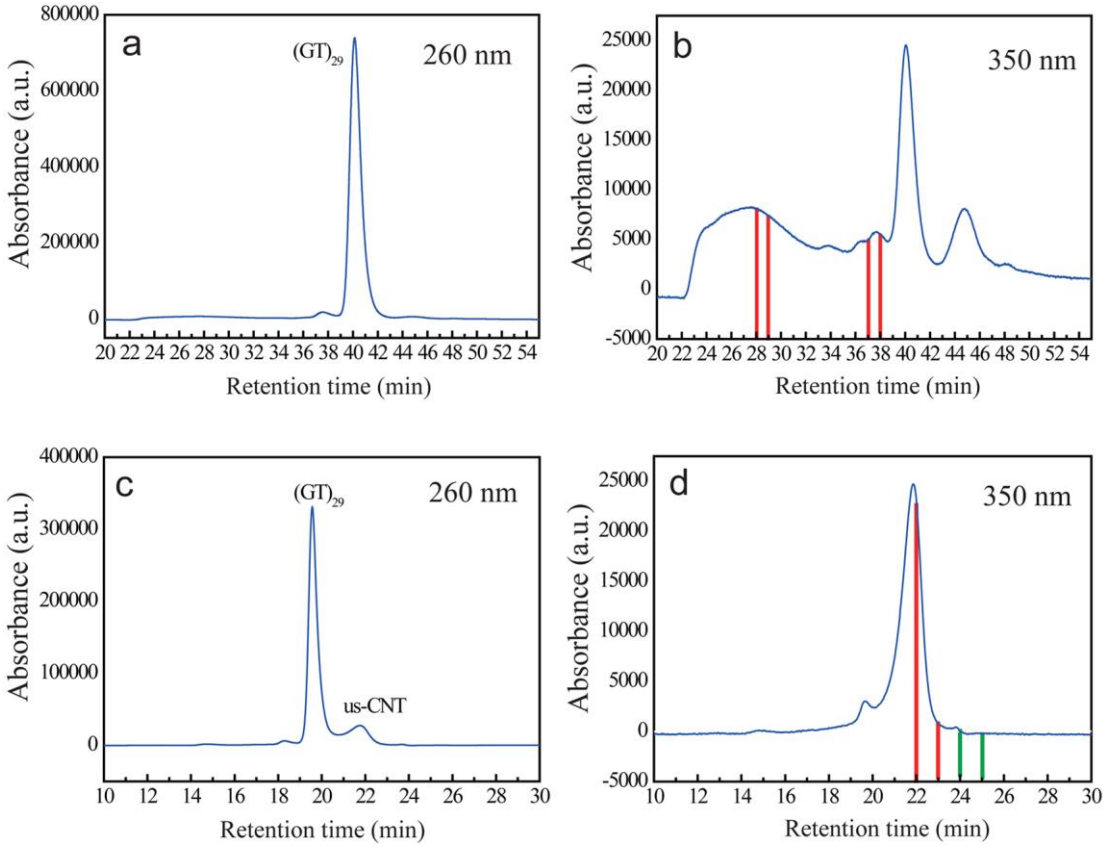

Supplementary Figure S2 | HPLC chromatogram of size exclusion separation of CNT1 and CNT2. a, Separation of CNT1 with detection UV wavelength of 260 nm. **b**, Separation of CNT1 with detection UV wavelength of 350 nm (×10 scale). The two fractions (28-29 min & 37-38 min) marked with red lines were taken for AFM measurements. **c**, Separation of CNT2 with detection UV wavelength of 260 nm. **d**, Separation of CNT2 with detection UV wavelength of 350 nm (×10 scale). The fraction of 22-23 min (marked with red lines) was taken for AFM and Raman measurements. The fraction of 24-25 min (marked with green lines) was the ONLY fraction that gave stable and reproducible nanopore current signals in single-channel recording experiments. The flow rate was 0.5 mL/min in **a** & **b**, 1.0 mL/min in **c** & **d**; and the injection volume was 0.5 mL in all HPLC experiments.

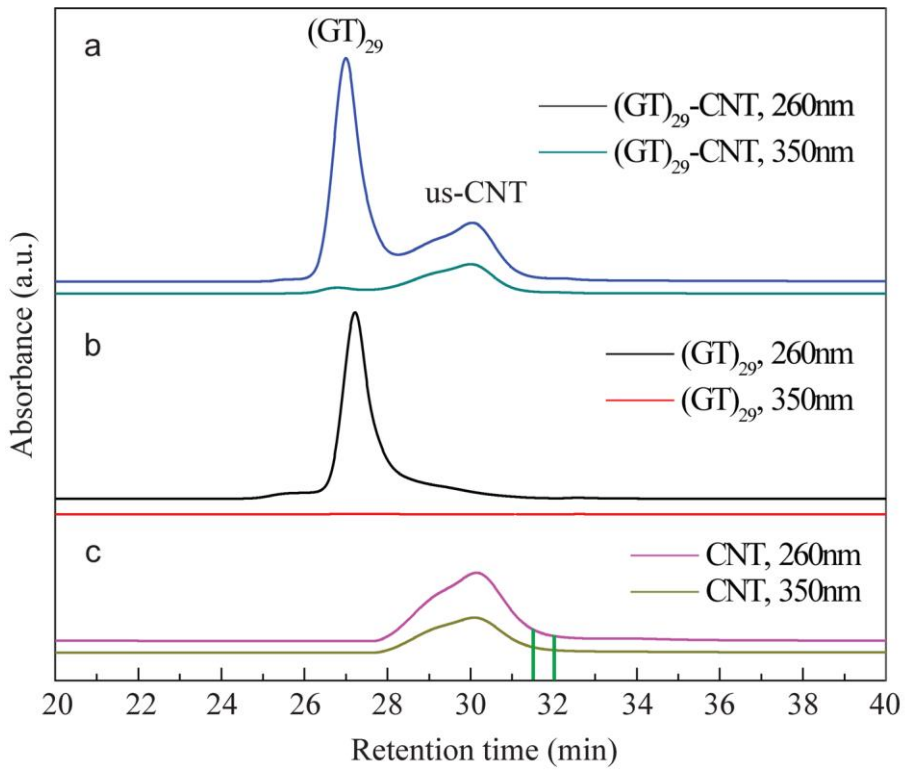

Supplementary Figure S3 | Merged HPLC chromatogram of separation of DNA-CNT2, DNA and CNT2. a, Separation of $(GT)_{29}$-CNT2 with detection UV wavelength of 260 and 350 nm. **b**, Separation of $(GT)_{29}$ with detection UV wavelength of 260 and 350 nm. **c**, Separation of CNT2 without DNA wrappings with detection UV wavelength of 260 and 350 nm. The fraction marked with green lines is the "active" fraction in single channel formation experiments. From comparison of the results, we could see that the very short SWCNTs did not have DNA coatings otherwise the DNA-CNT hybrid would be eluted before $(GT)_{29}$. Also, it was shown in an earlier report[47] that the pitch of DNA-SWCNTs is about 16.2 ± 1.5 nm. This value is much larger than the length of SWCNTs in the "active" HPLC fraction (5-10 nm). This also supports our claim that the ultrashort SWCNTs may not have DNA wrappings.

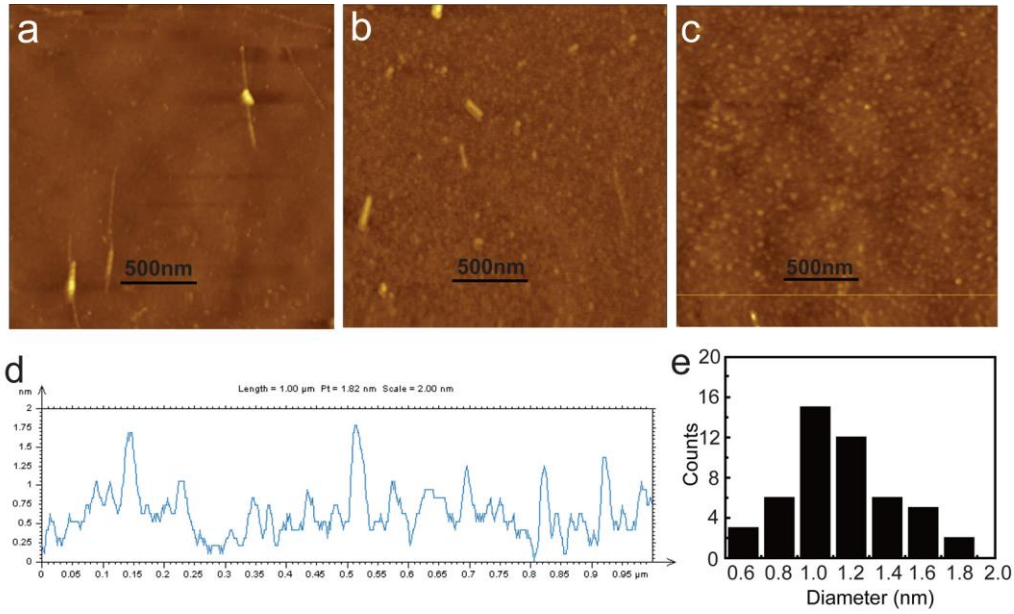

Supplementary Figure S4 | AFM characterization of SWCNTs. a, AFM image of the 28-29 min HPLC fraction of Supplementary Figure S2b. The nanotube length range: 450 nm-700 nm. **b**, AFM image of the 37-38 min HPLC fraction of Supplementary Figure S2b. The nanotube length range: 75 nm-200 nm. **c**, AFM image of the 22-23 min HPLC fraction of Supplementary Figure S2d. The average tube length is 11.4 nm (longest, 27.0 nm, shortest 3.0 nm). **d**, A cross section analytic curve of the yellow line section in image (**c**). **e**, Height histogram of the ultrashort SWCNTs on the yellow line in image **c**.

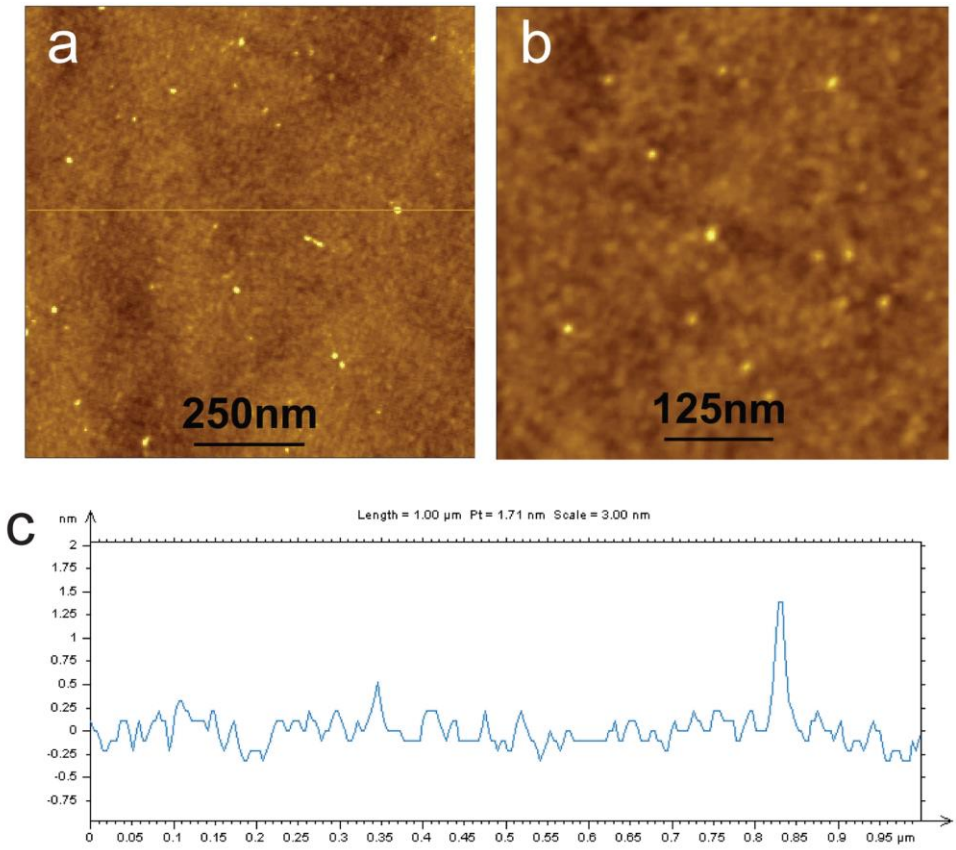

Supplementary Figure S5 | AFM characterization of the ultrashort SWCNTs. a-b, High resolution AFM image of the 24-25 min HPLC fraction of Supplementary Figure S2d [scanning area: 1.0 μm (**a**); 500 nm (**b**)]. **c,** A cross section analytic curve of the yellow line section in image **a**. The diameter of the nanotube is 1.3 nm. Two types of super-sharp AFM tips (SuperSharpSilicon™ tips from NanoSensors; tip radius 2.0 nm and Carbon Nanotube probe from AppMaterials Inc.; tip radius 2.0 nm) were used to perform length measurements of the ultrashort SWCNTs ("active fraction"). The average length of 50 randomly selected SWCNTs in this fraction is 5.3 nm (longest, 13.9 nm, shortest 1.0 nm with tip correction).

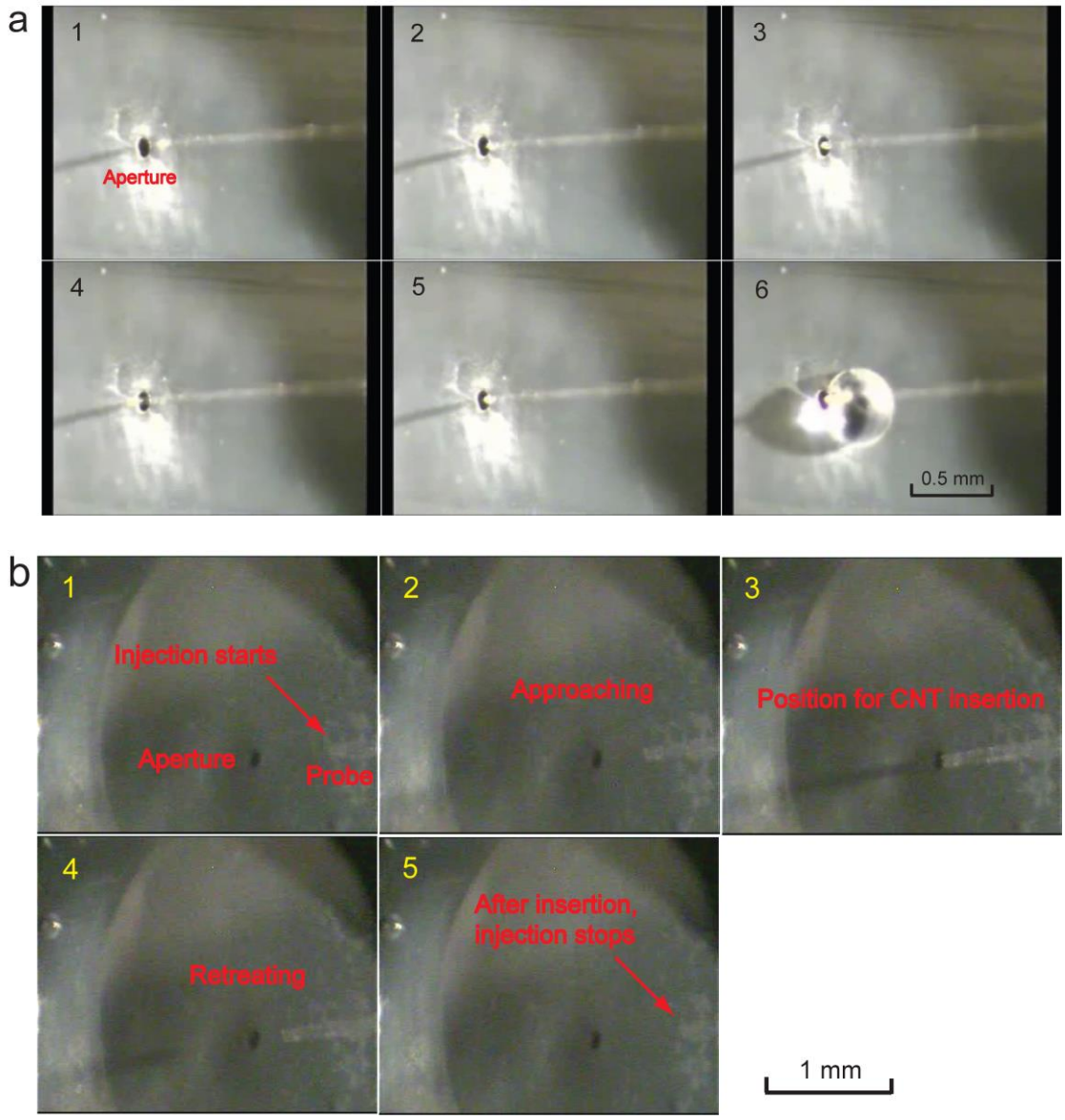

Supplementary Figure S6 | Insertion of SWCNTs into lipid bilayer with micro-injection probe. a, A series of snapshots from a video illustrate how the micro-injection probe moves close to the aperture, penetrates through the aperture, and then moves back, and finally injects solution from the needle. There is no buffer solution in the chamber. **b**, A series of snapshots from a video show how the probe gets SWCNTs inserted into lipid bilayer. The glass probe is behind the polycarbonate film. The videos of Supplementary Figure S6 were attached separately.

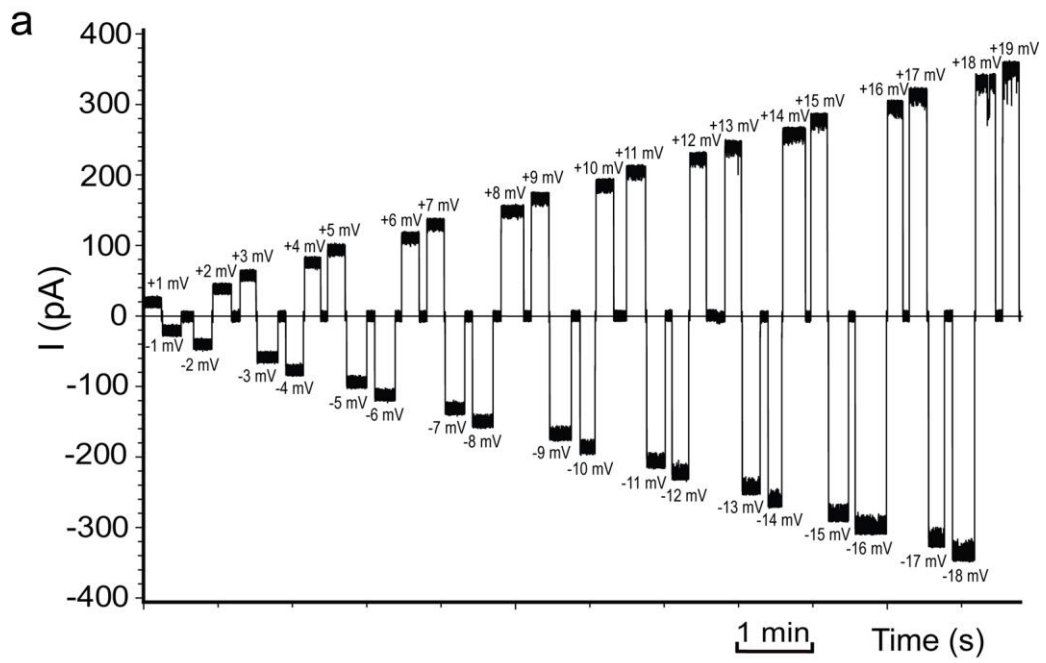
a
400
300
200
100
0
-100
-200
-300
-400
I (pA)
+1 mV
-1 mV
+2 mV
-2 mV
+3 mV
-3 mV
+4 mV
-4 mV
+5 mV
-5 mV
+6 mV
-6 mV
+7 mV
-7 mV
+8 mV
-8 mV
+9 mV
-9 mV
+10 mV
-10 mV
+11 mV
-11 mV
+12 mV
-12 mV
+13 mV
-13 mV
+14 mV
-14 mV
+15 mV
-15 mV
+16 mV
-16 mV
+17 mV
-17 mV
+18 mV
-18 mV
+19 mV
1 min
Time (s)

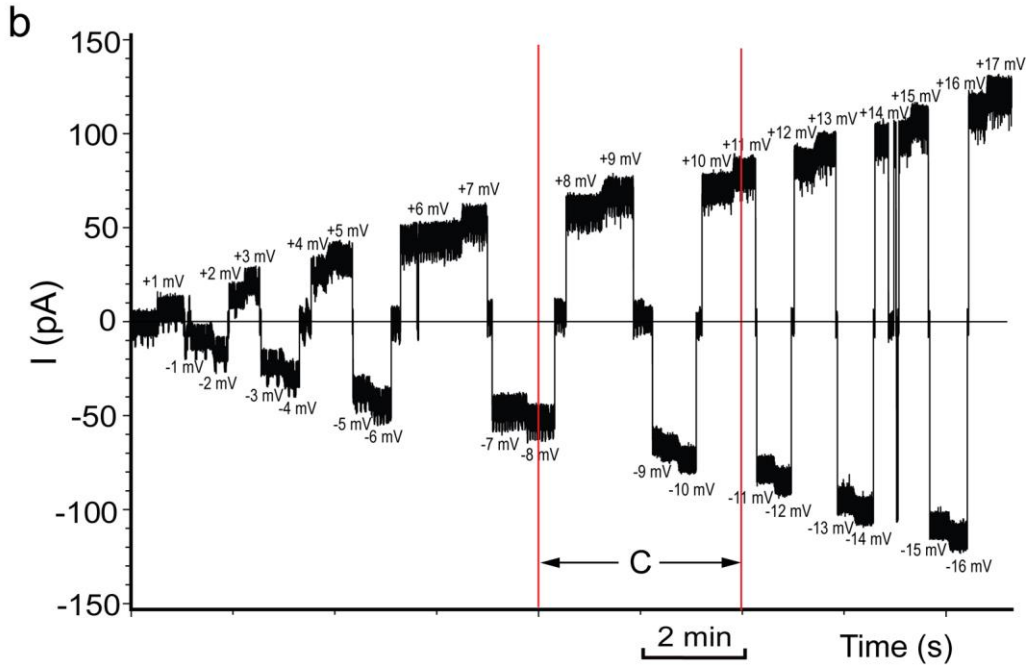
b
150
100
50
0
-50
-100
-150
I (pA)
+1 mV
-1 mV
+2 mV
-2 mV
+3 mV
-3 mV
+4 mV
-4 mV
+5 mV
-5 mV
+6 mV
-6 mV
+7 mV
-7 mV
+8 mV
-8 mV
+9 mV
-9 mV
+10 mV
-10 mV
+11 mV
-11 mV
+12 mV
-12 mV
+13 mV
-13 mV
+14 mV
-14 mV
+15 mV
-15 mV
+16 mV
-16 mV
+17 mV
C
2 min
Time (s)

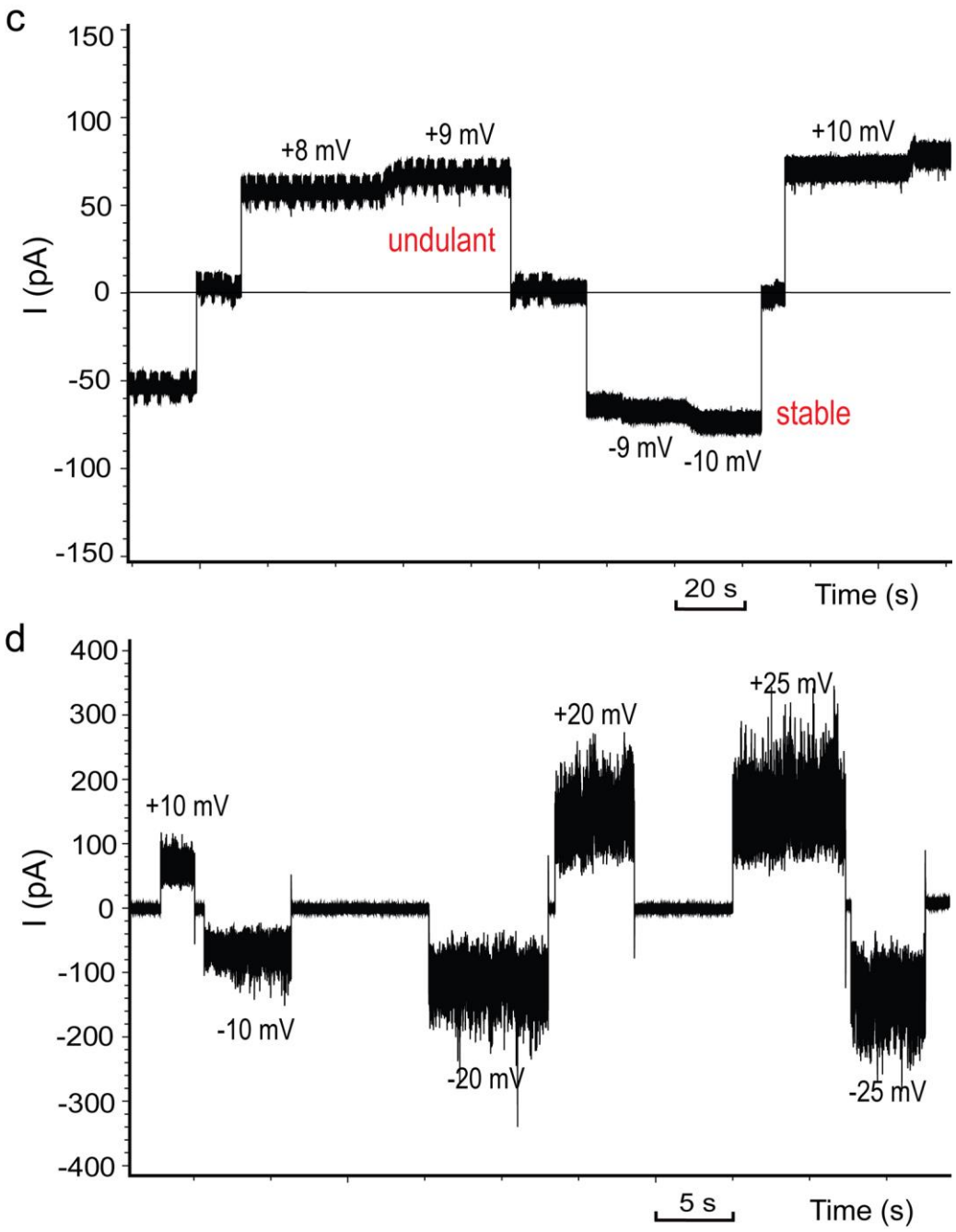

Supplementary Figure S7 | Insertion of different SWCNTs into lipid bilayer membrane. **a**, Stable current signal of an inserted SWCNT under different potentials. **b**, Current transition of one inserted SWCNT from undulant signals to stable signals. **c**, Expanded area in (**b**) marked with red lines. **d**, Unstable current signal of an inserted SWCNT under different potentials. All experiments were carried out in the buffer of 1 M KCl and 10 mM Tris, pH 8.0.

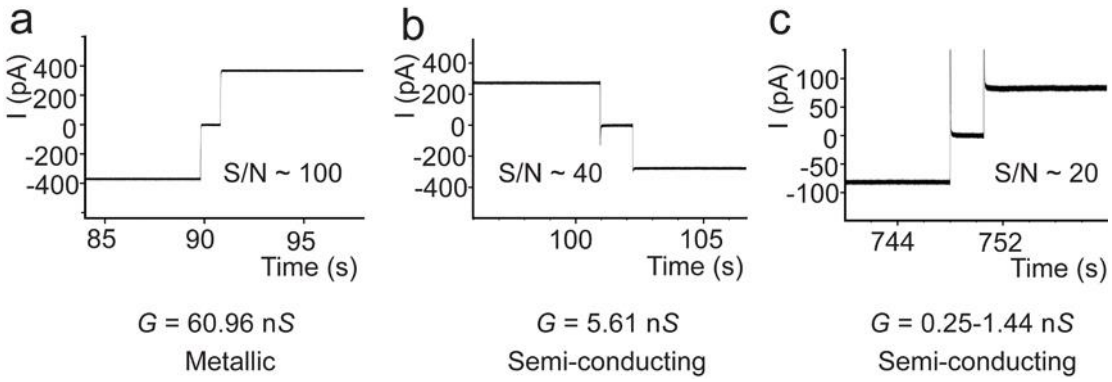

Supplementary Figure S8 | Representation of single channel recording traces of three typical SWCNT nanopores. a, Current trace of a metallic SWCNT nanopore with the transmembrane potential of 6.0 mV (Fig. 2a and 2d group 1). The conductance of the nanopore is 60.96 n*S*. **b**, Current trace of a semi-conducting SWCNT nanopore with the transmembrane potential of 40.0 mV (Fig. 2b and 2d group 2). The conductance of the nanopore is 5.61 n*S*. **c**, Current trace of a semi-conducting SWCNT nanopore with nonlinear I-V curve with the transmembrane potential of 180 mV (Fig. 2c and 2d group 3). The conductance range of the nanopore is 0.25-1.44 n*S*. All the traces were stable during the recording process which typically lasted for 4-6 hours. S/N is the signal-to-noise ratio.

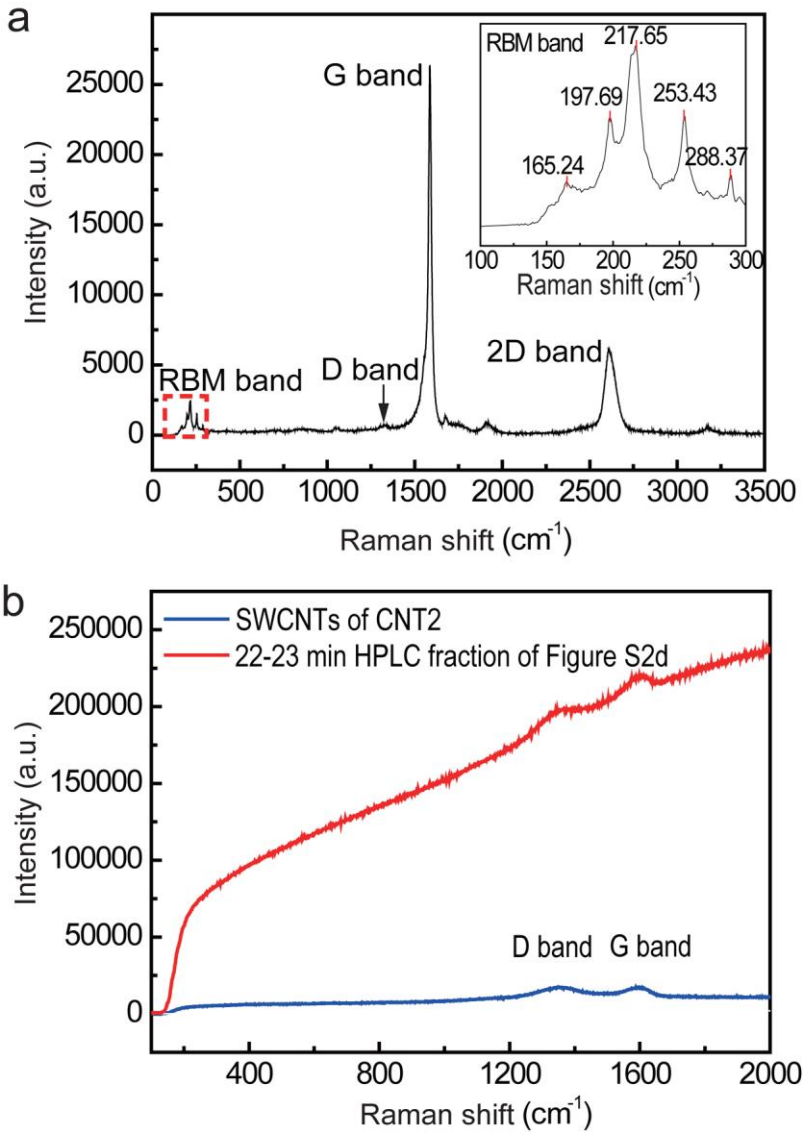

Supplementary Figure S9 | **Raman characterization of SWCNTs. a**, The Raman spectrum of uncut purified SWCNTs under 632.8 nm excitation. Inset: Magnified image of the radial breathing mode (RBM) regions in red dash line square. **b**, Raman spectra of the samples of CNT2 (blue line) and the 22-23 min HPLC fraction in Supplementary Figure S2d (red line). The D/G ratio, which represents the level of functionalization on carbon nanotubes, increases in both shortened SWCNTs. The HPLC fraction sample (red) shows high fluorescence background.

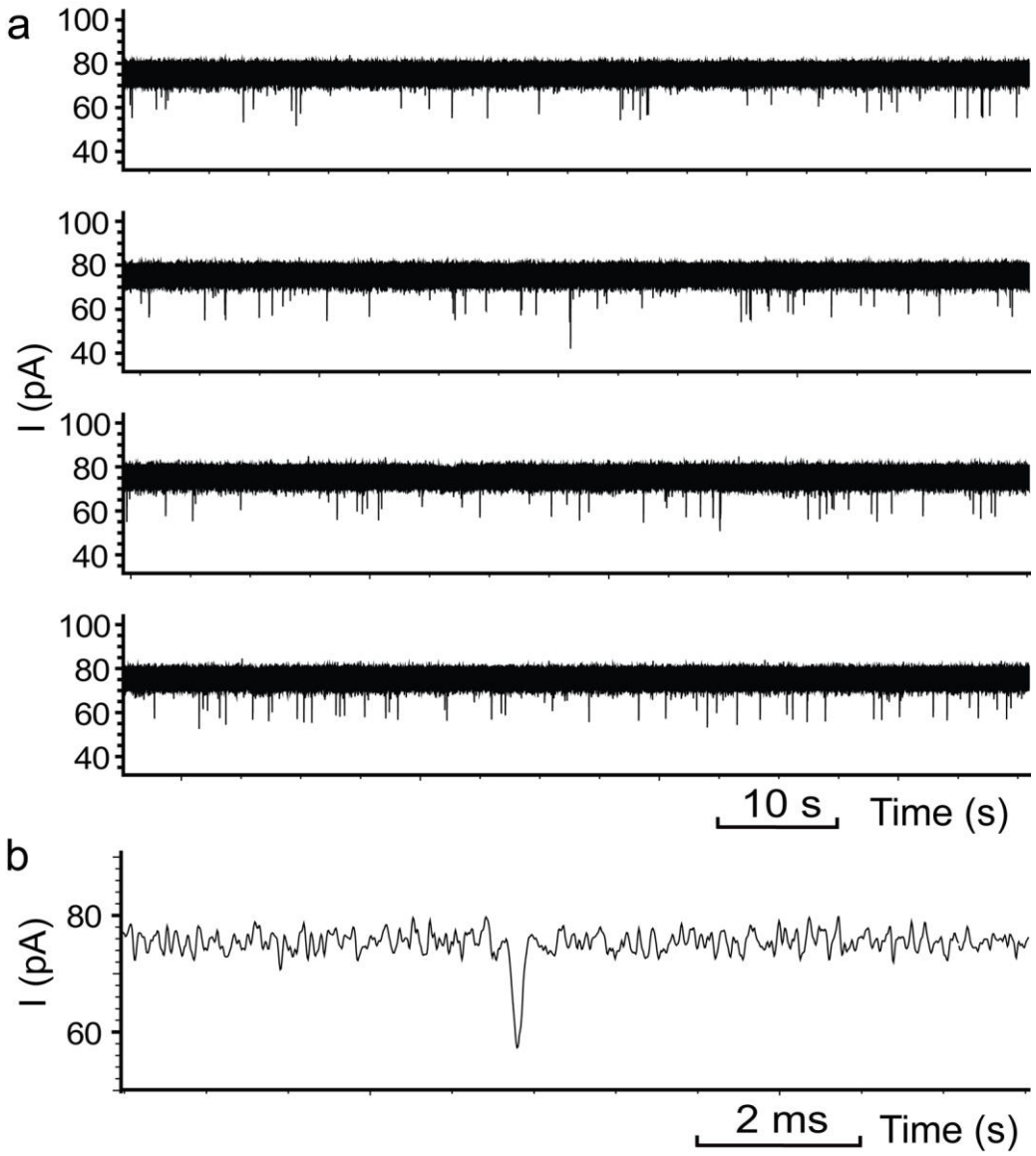

Supplementary Figure S10 | Current events of DNA1 colliding with SWCNT nanopores. **a**, Transient current signals of about 20 pA in amplitude appeared after DNA1 was added in the *cis* side. Buffer conditions: 1 M KCl and 10 mM Tris, pH 8.0, with the transmembrane potential held at +30 mV. **b**, Expanded view of a typical event. Those events do not represent DNA translocation through SWCNT nanopores as the qPCR sample collected in the *trans* side gave negative results.

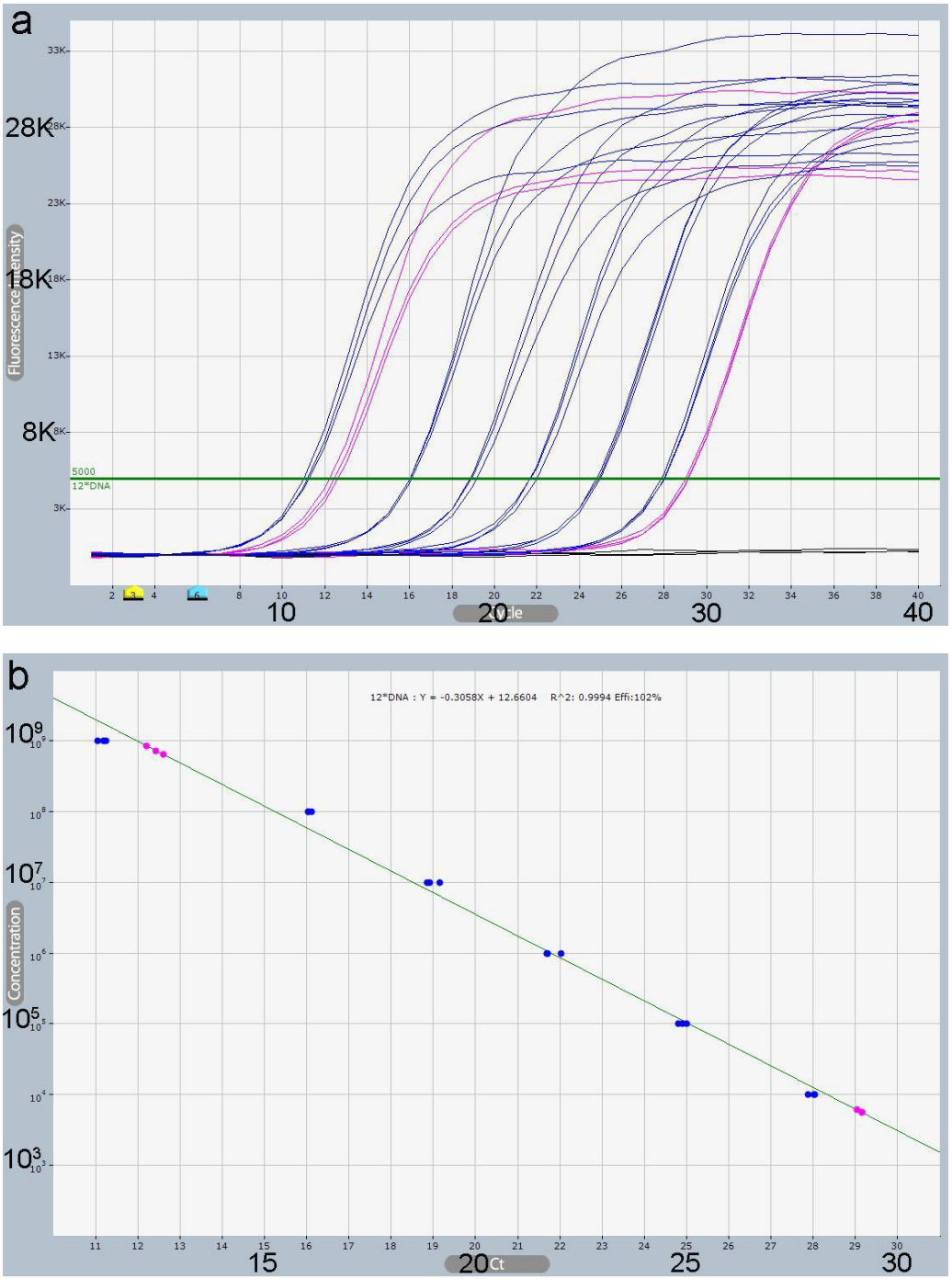

Supplementary Figure S11 | Quantitative PCR analysis of DNA1 translocation events. a, Amplification curves of the dilution series and samples were run in triplicate (blue lines). Two positive samples (purple lines) and the control sample (black lines) were also repeated three times. **b**, A standard curve with DNA concentration (copy numbers) plotted against the cycle threshold. Y = -0.3058X + 12.6604; R^2: 0.9994; Effi: 102%. The left purple dots represent the leaky membrane group; the right purple dots represent the large-current-blockade group. The DNA copy number difference between these two groups is about 10^5.

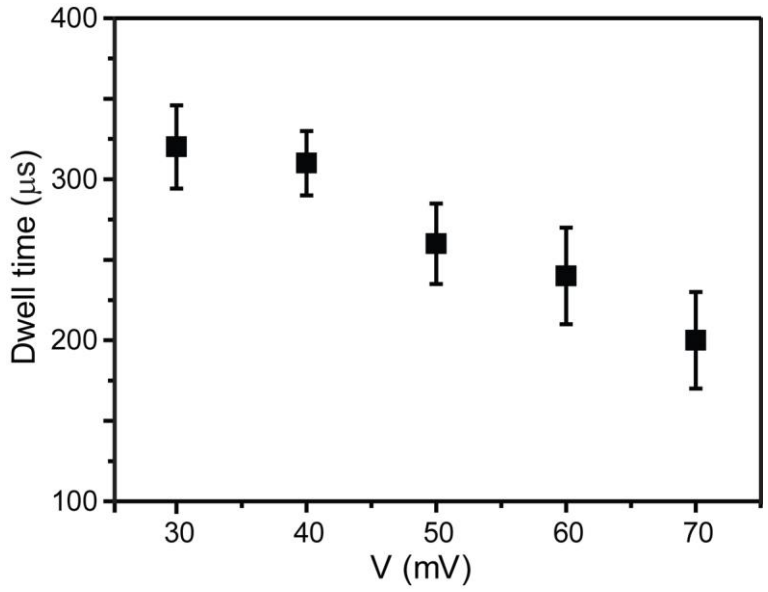

Supplementary Figure S12 | Plot of dwell time *versus* applied voltage for DNA translocation through SWCNT nanopores. Dwell time (τ) was obtained by a monoexponential fit to the dwell time histogram. All experiments were carried out in the buffer of 1 M KCl and 10 mM Tris, pH 8.0 (number of individual experiments n = 3). The conductances of the pores used in Supplementary Figure S12 are 8.73 n*S*, 9.08 n*S*, and 9.60 n*S*. The trend of dwell time decreasing along with the increase of voltage is similar to that in αHL and SS-nanopores. We limited the conductance range of SWCNTs between 8.0 and 25.0 n*S* in DNA translocation studies because we found that the results obtained within this range were highly reproducible. It should be noted that the conductance value of the nanotube *per se* does not have a prominent effect on the duration of DNA translocation.

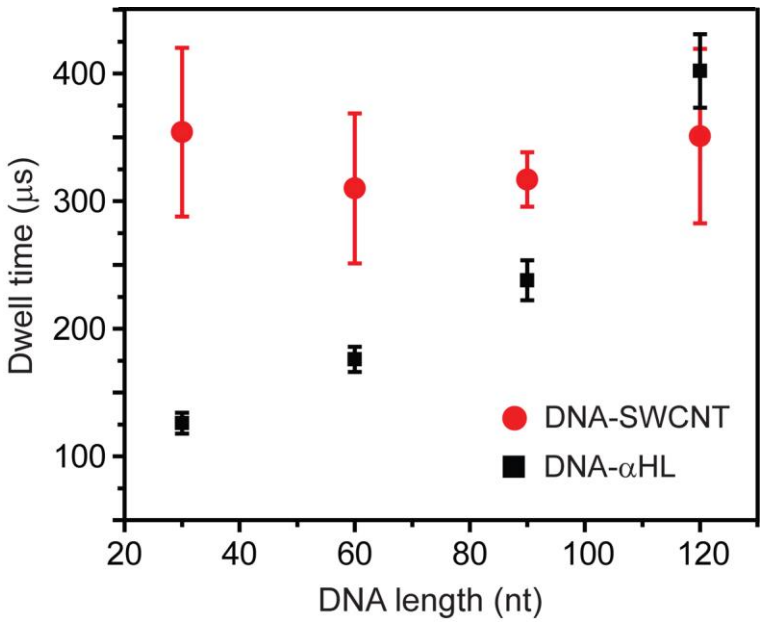

Supplementary Figure S13 | Comparison of dwell time of ssDNA translocation through SWCNT nanopores and αHL pore. Four DNAs of different length were used to conduct the translocation experiments in SWCNT nanopores: DNA1, 120nt; DNA6, 90nt; DNA7, 60nt; DNA8, 30nt (for sequences see Supplementary Table S2). Data were acquired in the buffer of 1 M KCl and 10 mM Tris, pH 8.0, with the transmembrane potential held at +40 mV for SWCNT nanopores and +100 mV for αHL (number of individual experiments n = 3). The large deviation of the SWCNT results is due to the fact that all the recordings were repeated in different SWCNTs (conductance range of the SWCNT nanopores: 8.0 - 25.0 n*S*). It is interesting to see that the duration of DNA translocation through SWCNT nanopore is almost independent of the length of DNAs, while in αHL it is a quasi-linear relationship. This might be because the rate-limiting step of DNA translocation process in SWCNTs is DNA escaping the nanopore[24], while the process of DNA sliding inside SWCNT takes very little time due to the nearly ideal slip boundary conditions[48].

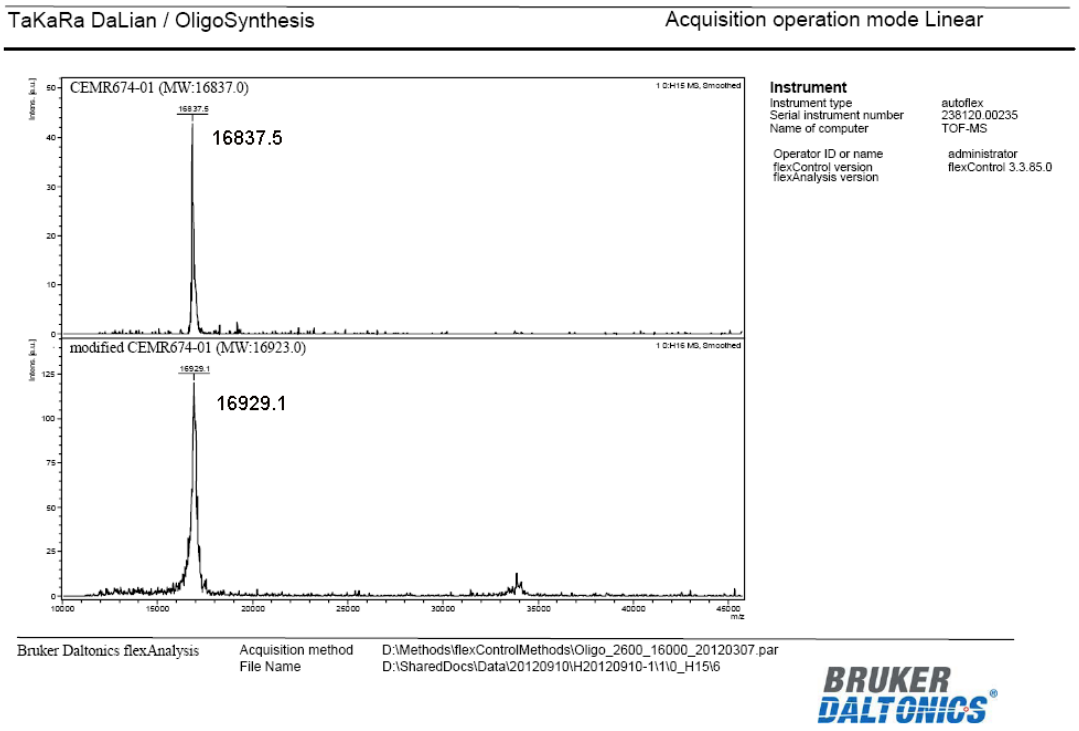

Supplementary Figure S14 | Mass spectrometry characterization of DNA2 and DNA2-Bzim. Top panel: MALDI-TOF of 5hmC-containing DNA2. Calculated molecular weight 16837.0; observed molecular weight 16837.5. Bottom panel: MALDI-TOF of 5hmC-containing DNA2-Bzim. Calculated molecular weight 16923.0; observed molecular weight 16929.1.

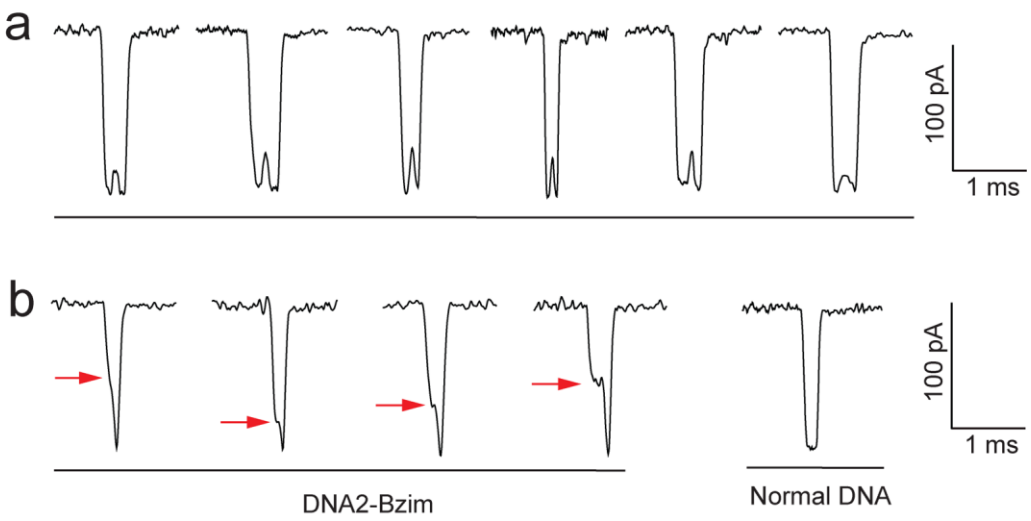

Supplementary Figure S15 | Comparison of current signature caused by DNA2-Bzim translocation through SWCNT nanopores and αHL. a, Typical characteristic current blockades in the presence of DNA2-Bzim recorded in different SWCNT nanopores. **b**, Current events caused by DNA2-Bzim translocation through αHL (left panel) and a "normal" DNA translocation event (right panel). The transient medium-level blockades prior to the DNA translocation level are marked by red arrows. Data were acquired in the buffer of 1 M KCl and 10 mM Tris, pH 8.0, with the transmembrane potential held at +40 mV for SWCNT nanopores and +140 mV for αHL; DNA2-Bzim final concentration 100 nM.

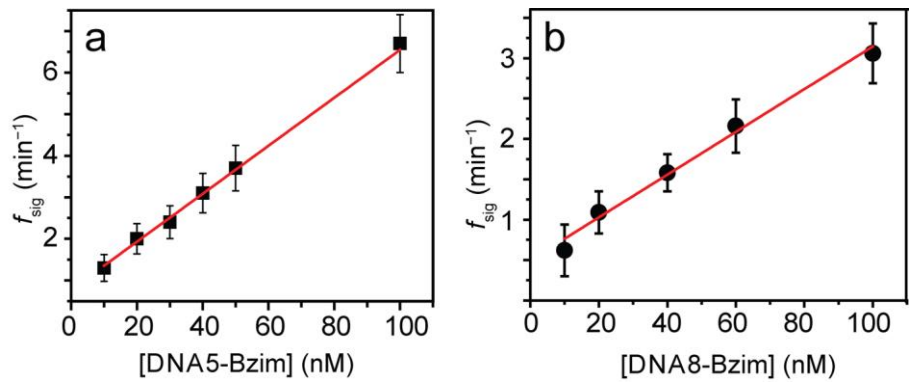

Supplementary Figure S16 | Correlation of f_{sig} with Bzim-DNA concentrations between 10 nM and 100 nM. a, Plot of f_{sig} versus DNA2-Bzim concentrations. **b**, Plot of f_{sig} versus DNA5-Bzim concentrations. The measurements of each modified DNA were conducted in the same SWCNT nanopore by gradually increasing the DNA concentration. All the data were acquired in the buffer of 1 M KCl and 10 mM Tris, pH 8.0, with the transmembrane potential held at +40 mV (number of experiments: 6 for **a** and 3 for **b**).

Supplementary Table S1 Calculated diameter (*d*), assigned chiralities (*n*, *m*) and electronic type from ω_{RBM} of 632.8 nm excitation in Supplementary Figure S9a.

$\omega_{RBM} \sim d$ (ref. 49)	Experim-ental ω_{RBM}	Reference[50-52] ω_{RBM}	Calcul-ated *d*	Reference[50-52] *d*	(*n*, *m*)	Electronic Type
$\omega_{RBM} = (223.5/d) + 12.5$	165.24	164.0	1.46	1.51	(11, 11)	metallic
	197.69	196.3	1.21	1.183	(14, 2)	metallic
		193.5		1.206	(13, 4)	
	217.65	217.4	1.09	1.077	(12, 3)	metallic
		212.4		1.111	(11, 5)	
	253.43	251.3	0.93	0.936	(10, 3)	semiconducting
		256.6		0.916	(9, 4)	
		256.6		0.916	(11, 1)	
	288.37	289.9	0.81	0.806	(9, 2)	semiconducting
		282.1		0.829	(7, 5)	

Supplementary Table S2 Sequences of studied DNA oligomers

DNA1	5’-CCTACCTATCCTTCCACTCATTTTCCTTAACCATTTCATTCACCCATC TCTTCACTCCATCTATCACCTCCATACATACCCTCCATATTACACTCCC ACT ACTCCTCACACTACCATACC-3’
DNA2	5’-TATCACCTCCATACAT**(5hmC)**GCTCCATATTACACTCCCACGA CTCCTCACACTACCATA-3’
DNA3	5’-TATCACCTCCATACAT**(5mC)**GCTCCATATTACACTCCCACGA CTCCTCACACTACCATA-3’
DNA4	5’-TATCACCTCCATACAT**C**GCTCCATATTACACTCCCACGA CTCCTCACACTACCATA-3’
DNA5	5’-TATCACCTCCATACAT**(5hmC)**GCTCCATATTACACTCCCACGA ACTCCC**(5hmC)**GACTCCTCACACTACCATA-3’
DNA6	5’-CCTACCTATCCTTCCACTCATTTTCCTTAACCATTTCATTCACCCA TCTCTTCACTCCATCTATCACCTCCATACATACCCTCCATATTA-3’
DNA7	5’-CCTACCTATCCTTCCACTCATTTTCCTTAACCATTTCATTCACCCATC TC TTCACTCCAT-3’
DNA8	5’-CCTACCTATCCTTCCACTCATTTTCCTTAA-3’

(5hmC)—5-hydroxymethylcytosine; **(5mC)**—5-methylcytosine

Supplementary Table S3. qPCR cycle protocol

Step	Function	Temperature	Time (hh:mm:ss)	Repeat
1	INCUBATE	95.00	0:5:0	0
2	INCUBATE	95.00	0:0:5	0
3	INCUBATE	60.00	0:0:30	0
4	SCAN			0
5	GO TO	Step 2		40
6	MELTING 65°C to 90°C, Every 1.0°C	1 Sec.		
7	INCUBATE	30.00	0:0:30	0
8	End			

Supplementary Methods

Atomic Force Microscopy (AFM).

We chose 3-aminopropyltriethoxysilane-coated SiO_2 on silicon as the substrate for AFM sample deposition, which was prepared as follows. Silicon chips were first cleaned with piranha solution (70 vol. % H_2SO_4 + 30 vol. % H_2O_2). Then, cleaned silicon chips were treated with 3-aminopropyltriethoxysilane (APTES) solution (5 mL ethanol, 200 μL acetic acid, 200 μL Milli-Q water, 100 μL APTES) for 30 minutes to facilitate the deposition of SWCNTs onto the substrate. SWCNTs were deposited by soaking a piece of SiO_2 in the HPLC solution for a period of time (for CNT1, ~30 min, for CNT2 ~10 s). The substrate was then rinsed briefly with water, dried with N_2, and imaged by tapping mode on AFM (Agilent 5500). About 50 ultrashort SWCNTs (CNT2) were measured to obtain the average length. AFM tip model: Bruker MPP-11100-10. We adopted a method in literature for AFM image tip correction in SWCNT length measurements[53]. This correction was especially important when the lengths of SWCNTs were in < 20 nm range. We measured the apparent width (W) and height (H) of SWCNTs by regular Si tips. The tip size can be calculated from the formula:

$$\text{Tip size} = 1/2(W-H)$$

This was used to correct the length of very short SWCNTs:

$$\text{True Length} = \text{Measured Length} - 2 * (\text{Tip size})$$

According to our measurements, a typical tip size is 11 ± 3 nm. The average length of 50 randomly selected SWCNTs in Supplementary Figure S4c (22-23 min HPLC fraction of Supplementary Figure S2d) is 11.4 nm (longest 27.0 nm; shortest 3.0 nm).

Raman spectra.

The samples were prepared by dropping the HPLC fraction onto a glass substrate and then dried using an electrical heater. The Raman spectra measurements (Model: Renishaw, RM2000) were carried out at 1.96 eV (632.8 nm) excitation at ×20 magnification and 5-μm spot size. Laser power of 4.7 mW was used to prevent destruction of the samples during measurement. Raman spectra indicated that the fractions of CNT2 have very few or no radial breathing modes. The SWCNT diameters calculated from Raman spectra (Supplementary Table S1) agree with the values obtained from AFM measurements.

Calculation of ionic current in SWCNTs.

By assuming a very simple model without any free energy barrier, the ionic conductance of electrolyte inside SWCNTs should be given by

$$G = 6.02 \times 10^{26} (\mu_K + \mu_{Cl}) c_{KCl} e \pi D_{CNT}^2 / 4 L_{CNT}$$

where $\mu_K = 7.62 \times 10^{-8}$ m^2/Vs and $\mu_{Cl} = 7.91 \times 10^{-8}$ m^2/Vs are the electrophoretic mobilities of potassium and chloride ions, respectively, c_{KCl} is the KCl concentration in mole/l, e the electronic charge, D_{CNT} the tube diameter, and L_{CNT} the tube length. For tube diameter of 1-2 nm and tube length of 5-10 nm, the calculated ionic conductance is between 1.18 and 9.40 n*S*.

Quantitative polymerase chain reaction (qPCR).

Quantification of translocated DNA is performed on Exicycler™ 96 (BIONEER, Shanghai). DNA was added in the *cis* side and samples were taken from the *trans* side at 60-minute intervals under a positive potential of 30 mV. The bilayer membrane was maintained intact during the whole process of translocation experiments. The merged samples were subject to centrifugal ultra-filtration (3 kD UFC900308; Millipore) to remove salt and buffer molecules. The washing and ultra-filtration were repeated 3 times before the sample was lyophilized to dryness for PCR amplification. Apart from samples taken from different translocation experiments, two additional control experiments were also performed, one without adding DNA in the *cis* and the other with DNA traversing from *cis* to *trans* in the presence of a broken bilayer membrane. Only the large blockades group and the leaky membrane group gave positive PCR results, confirming that the large-amplitude blockades are attributable to DNA translocation through SWCNT nanopores (Supplementary Figure S11). Additionally, the difference of the number of DNA copies between these two groups is well in line with literature results[54]. The amplification mixture consisted of forward primer (CCTACCTATCCTTCCACTC, 1 μL), Reverse primer (GGTATGGTAGTGTGAGG 1 μL), template (DNA1 120bp, 4 μL), GreenStar Real-Time PCR MasterMix x2, 25 μL and Milli-Q water (19 μL).

Supplementary References

47. Gao, X. *et al.* Detection of trace Hg^{2+} via induced circular dichroism of DNA wrapped around single-walled carbon nanotubes. *J. Am. Chem. Soc.* **130**, 9190-9191 (2008).
48. Sokhan, V. P., Nicholson, D. & Quirke, N. Fluid flow in nanopores: Accurate boundary conditions for carbon nanotubes. *J. Chem. Phys.* **117**, 8531-8539 (2002).
49. Bachilo, S. M. *et al.* Structure-assigned optical spectra of single-walled carbon nanotubes. *Science* **298**, 2361-2366 (2002).
50. Weisman, R. B. & Bachilo, S. M. Dependence of optical transition energies on structure for single-walled carbon nanotubes in aqueous suspension: An empirical Kataura plot. *Nano Lett.* **3**, 1235-1238 (2003).
51. Maultzsch, J., Telg, H., Reich, S. & Thomsen, C. Radial breathing mode of single-walled carbon nanotubes: Optical transition energies and chiral-index assignment. *Phys. Rev. B* **72**, 205438 (2005).
52. Jorio, A. *et al.* Structural (n, m) determination of isolated single-wall carbon nanotubes by resonant Raman scattering. *Phys. Rev. Lett.* **86**, 1118-1121 (2001).
53. Sun, X. *et al.* Optical properties of ultrashort semiconducting single-walled carbon nanotube capsules down to sub-10 nm. *J. Am. Chem. Soc.* **130**, 6551-6555 (2008).
54. Wendell, D. *et al.* Translocation of double-stranded DNA through membrane-adapted phi29 motor protein nanopores. *Nat. Nanotechnol.* **4**, 765-772 (2009).